

The Bussgang algorithm for multichannel blind image restoration

*Giampiero Panci***, *Patrizio Campisi**, *Stefania Colonnese***, *Gaetano Scarano***

**Dip. INFOCOM, Università di Roma "La Sapienza"
via Eudossiana 18, I-00184 Roma, Italy
Tel:+39.6.4458.5500, Fax:+39.6.4873.300,
e-mail: (scarano,colonnese,panci)@infocom.uniroma1.it

*Dip. Ingegneria Elettronica, Università di Roma Tre
via della Vasca Navale 84, I-00146 Roma, Italy
Tel:+39.6.5517.7064, Fax:+39.6.5579.078,
e-mail: campisi@ele.uniroma3.it

ABSTRACT

This work derives the multichannel Bussgang restoration algorithm for blind image restoration problems. In its basic outline, the derived Bussgang restoration algorithm is based on iteratively filtering the measurements by means of a bank of FIR filters, and updating the filter-bank on the base of a nonlinear estimate of the original image. The filters are updated by solving a linear system (*multichannel normal equations*) whose coefficients' matrices depend on the cross-correlations between the measurements and a nonlinear estimate of the original image, this latter obtained using a Bayesian criterion. Experimental results pertaining to restoration of motion blurred text images and out-of-focus star field images are reported.

1 Introduction

Image restoration, aiming at recovering an original image observed through a single or multiple noisy channels, has been widely studied in literature because of its theoretical as well as practical importance [1], [2], [3].

In some situations the blur is assumed known, which leads to well known deconvolution methods such as Wiener filtering, recursive Kalman filtering, constrained iterative deconvolution methods.

However, in many practical situations, the blur is partially known [4] or unknown, because an exact knowledge about the mechanism of the degradation process is not available. Therefore, the blurring process needs to be characterized on the available blurred data. In such a scenario, blind image restoration techniques are employed. They aim at the retrieval of an original image, observed through a non-ideal channel, whose characteristics are not known, or are partially known, in the restoration phase.

In some applications (*e.g.* electron microscopy, remote sensing, tele-surveillance) the observation system yields multiple observation of the original image and, in line of principle, the restoration algorithm can exploit the redundancy of the observations in order to achieve performance unobtainable from a single measure [5], [6].

In this paper, the multichannel Bussgang restoration algorithm is derived, thus extending the single-channel Bussgang restoration algorithm [7, 8, 9]. The algorithm is iterative and the generic iteration can be summarized as follows. The restored image is obtained at the output of a bank of FIR filters that act on the multiple observations. Then, from this "linear" estimate, a different "nonlinear" estimate is obtained according to a Bayesian Minimum Mean Square Error (MMSE) criterion that exploits a suitable stochastic model of the image to be restored. Finally, the nonlinear estimate is used to form the cross-correlations needed in the r.h.s. of the multichannel normal equations (Wiener) that solve for the updated impulse responses of the filter-bank. The algorithm is started using a suitable initial guess of the deconvolution filter-bank. Often, the neutral choice of 2-D unit sample filters is sufficient for the convergence.

We remark the key role played by the nonlinear estimation, which drives the algorithm toward an equilibrium point where the deconvolved image is congruent with the assumed stochastic model. In other words, the "quality" of the deconvolved image is determined almost exclusively by the nonlinear estimation.

The deconvolution algorithm is here applied to two restoration experiments, concerning with the recovery of motion blurred text images and of out-of-focus star field (bright and dark spots) images.

2 Observation model

The single-input multiple-output (SIMO) observation model of images is depicted in Fig.1 and analytically characterized by:

$$y_i[m, n] = (x * h_i)[m, n] + v_i[m, n], \quad (1)$$

for $i = 0, \dots, M - 1$. The additive terms $v_i[m, n]$ represent realizations of mutually uncorrelated zero mean white Gaussian processes.

The restored image $\hat{x}[m, n]$ is obtained from the observations $y_i[m, n]$ by means of a bank of M linear FIR restoration filters $f_i[m, n]$, $i = 0, \dots, M - 1$, whose sup-

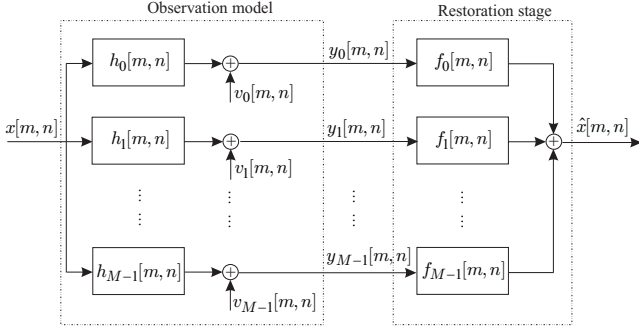


Figure 1: *Blurred image generation model and restoration stage.*

port is $(2P + 1 \times 2P + 1)$, namely:

$$\hat{x}[m, n] = \sum_{i=0}^{M-1} \sum_{t, u=-P}^P f_i[t, u] y_i[m-t, n-u] \quad (2)$$

3 Multichannel Wiener filtering

In this Section the multichannel Wiener filtering is described. The results obtained hereafter will be used in the next Section. Specifically, with reference to the observation model depicted in Fig.1, the Wiener filter-bank $f_i[m, n], i = 0, \dots, M-1$, minimizes the MSE of the linear estimate given by (2), given by:

$$\text{MSE}(f_1, \dots, f_{M-1}) \stackrel{\text{def}}{=} E\{|\hat{x}[m, n] - x[m, n]|^2\} \quad (3)$$

Applying the orthogonality principle to the minimization of the above cost function yields the following linear set of $(M \times 2P + 1 \times 2P + 1)$ *normal equations* for the determination of the $(M \times 2P + 1 \times 2P + 1)$ coefficients of the multichannel Wiener filter

$$\sum_{j=0}^{M-1} \sum_{t, u=-P}^P R_{y_j y_i}[r-t, s-u] f_j[t, u] = R_{x y_i}[r, s] \quad (4)$$

being

$$R_{y_j y_i}[r, s] \stackrel{\text{def}}{=} E\{y_j[m, n] y_i[m-r, n-s]\}$$

$$R_{x y_i}[r, s] \stackrel{\text{def}}{=} E\{x[m, n] y_i[m-r, n-s]\}$$

with $i = 0, \dots, M-1$, and $r, s = -P, \dots, P$.

Deconvolution by Wiener filtering requires, in principle, the knowledge of the cross-correlations between the original image and the measurements; it provides the optimal linear estimate of the original image in the MMSE sense. If such cross-correlation is not available, one can resort to a suitable estimate, as in the multichannel Bussgang blind deconvolution algorithm described below.

4 Multichannel Bussgang Algorithm

The Bussgang approach of HOS based methods [7, 8, 9] is here extended to the multichannel blind image

restoration problem. We derive the multichannel Bussgang blind deconvolution algorithm on the base of the following facts:

- The cross-correlations in the r.h.s. of (4) can be expressed in terms of the conditional a posteriori mean $\hat{x}[m, n] \stackrel{\text{def}}{=} E\{x[m, n]/y_0, \dots, y_{M-1}\}$ as follows:

$$R_{x y_i}[r, s] = E\{\hat{x}[m, n] y_i[m-r, n-s]\} = R_{\hat{x} y_i}[r, s]$$

The conditional a posteriori mean constitutes also the MMSE estimate of $x[m, n]$ given the observed samples of the sequences y_0, \dots, y_{M-1} .

- Hence, the multichannel Wiener filter-bank $f_i[m, n]$ is obtained by solving the normal equations (4) after having substituted $R_{\hat{x} y_i}[r, s] = R_{x y_i}[r, s]$ in the r.h.s. of (4), for $i = 0, \dots, M-1$.
- The deconvolved image $\hat{x}[m, n]$ at the output of the Wiener filter-bank is a sufficient statistic for the estimation of $x[m, n]$ given y_0, \dots, y_{M-1} ; therefore we have also $\hat{x}[m, n] = E\{x[m, n]/\hat{x}\}$

Inspired by this analysis we devise an iterative blind deconvolution algorithm whose k -th iteration is here summarized:

1. the linear estimate $\hat{x}^{(k)}[m, n]$ is computed from the observed sequences y_0, \dots, y_{M-1} by means of a previous estimate of the Wiener filter-bank $f_i^{(k-1)}$, *i.e.*

$$\hat{x}[m, n] = \sum_{i=0}^{M-1} (f_i^{(k-1)} * y_i)[m, n]$$

Since the original image can be retrieved except for an amplitude scale factor, at each iteration the Wiener filter-bank is normalized to yield an unitary energy output.

2. according to a suitable stochastic model of the image $x[m, n]$, the nonlinear MMSE estimate $\tilde{x}^{(k)}[m, n]$ is computed as

$$\tilde{x}^{(k)}[m, n] = \eta(\hat{x}^{(k)}) \stackrel{\text{def}}{=} E\{x[m, n]/\hat{x}^{(k)}\}$$

In general, the nonlinear estimator $\eta(\cdot)$ exhibits non-zero spatial memory.

3. a new estimate of the Wiener filter-bank $f_i^{(k)}$ is computed by solving the normal equations (4) where $R_{y_j y_i}[r, s]$ and $R_{\tilde{x} y_i}[r, s]$ are substituted by their sample estimates $\hat{R}_{y_j y_i}[r, s]$ and $\hat{R}_{\tilde{x}^{(k)} y_i}[r, s]$, respectively. Note that in this step only the cross-correlations $\hat{R}_{\tilde{x}^{(k)} y_i}[r, s]$ are computed, while $\hat{R}_{y_j y_i}[r, s]$ are computed only once before starting the iterations.
4. convergence is tested by a suitable criterion.

The algorithm is initialized by a suitable initial guess $f_i^{(0)}[m, n], i = 0, \dots, M-1$, of the Wiener filter-bank.

As outlined in [7, 8], the iterative algorithm reaches an equilibrium point, namely $f_i^{(k-1)}[m, n] = f_i^{(k)}[m, n]$,

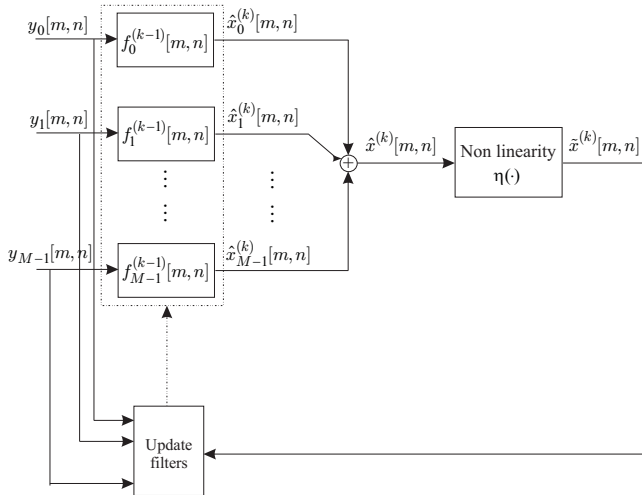


Figure 2: General form of the Bussgang deconvolution algorithm.

when the cross-correlations between the linearly restored image $\hat{x}^{(k)}[m, n]$ and the measured images $y_i[m, n]$, $i = 0, \dots, M - 1$, reproduce, within an amplitude scale factor, the cross-correlations between the estimate $\tilde{x}^{(k)}[m, n]$ and the observations, that is:

$$R_{\tilde{x}y_i}[r, s] = \text{const} \cdot R_{\hat{x}y_i}[r, s]. \quad (5)$$

Since the equilibrium point is characterized by the invariance between cross-correlations (5), also known as ‘‘Bussgang’’ property of stationary processes under nonlinear transformations, the deconvolution algorithm is commonly referred to as ‘‘Bussgang’’ deconvolution algorithm [7, 8]. However, it is well known that if the original image $x[m, n]$ is a realization of a stationary Gaussian random field, the restoration process becomes inherently ambiguous, being the Bussgang property satisfied irrespective of the filter-bank $f_i[m, n]$.

A discussion on the convergence of the algorithm is reported in [10] for the case of single channel.

We must remark that the convergence of the algorithm is affected by the nonlinearity $\eta(\cdot)$, whose analytical determination can result quite difficult. However, if the residual error at the k -th iteration $w^{(k)}[m, n] = \hat{x}^{(k)}[m, n] - x[m, n]$ can be assumed independent of $x[m, n]$, the nonlinearity $\eta(\cdot)$ has zero spatial memory and it depends only on the marginal probability density function (pdf) $p_x(\cdot)$ of $x[m, n]$ and on the marginal pdf $p_{w^{(k)}}(\cdot)$ of the residual error $w^{(k)}[m, n]$. This assumption is reasonable when the iterative deconvolution is close to the convergence, where the residual noise can be approximated with a zero mean white Gaussian process of variance $\sigma_{w^{(k)}}^2$.

For instance, in the case of binary text images the image $x[m, n]$ can be stochastically described as a realization of a white stationary random field with pdf

$$p_x(x) = p_0\delta(x) + (1 - p_0)\delta(x - 1) \quad (6)$$

The MMSE estimate $\tilde{x}^{(k)}$, given $\hat{x}^{(k)}$, turns out to be:

$$\tilde{x}^{(k)} = \eta(\hat{x}^{(k)}) = \frac{1}{1 + \frac{p_0}{1 - p_0} \exp\left(-\frac{\hat{x}^{(k)} - \frac{1}{2}}{\sigma_{w^{(k)}}^2}\right)} \quad (7)$$

Another interesting case are star field images, *i.e.* images characterized by an excitation field made of sparse bright or dark spots in a gray background. In this case, we can model the pdf of the image according to the following Gaussian mixture:

$$p_x(x) = p_0\delta(x) + (1 - p_0)\mathcal{N}(x, 0, \sigma_x^2) \quad (8)$$

where $\mathcal{N}(x, m_x, \sigma_x^2)$ denotes the Gaussian pdf with mean m_x and variance σ_x^2 . This case closely resembles the geophysical prospecting problem addressed in [7], where the nonlinear estimate $\tilde{x}^{(k)}$ has been calculated as follows:

$$\tilde{x}^{(k)} = \eta(\hat{x}^{(k)}) = \frac{\sigma_{\hat{x}^{(k)}}^2}{\sigma_{\hat{x}^{(k)}}^2 + \sigma_{w^{(k)}}^2} \cdot \frac{\hat{x}^{(k)}}{g(\hat{x}^{(k)})} \quad (9)$$

being the function $g(\cdot)$ given by:

$$g(x) = 1 + \frac{p_0}{1 - p_0} \sqrt{1 + \frac{\sigma_{\hat{x}^{(k)}}^2}{\sigma_{w^{(k)}}^2}} \exp\left(-\frac{\frac{x^2}{2\sigma_{\hat{x}^{(k)}}^2}}{1 + \frac{\sigma_{\hat{x}^{(k)}}^2}{\sigma_{w^{(k)}}^2}}\right)$$

5 Experimental Results and Final Remarks

Experimentations have been performed on synthetically generated binary text images and star fields. In Fig.3 the original test images before application of the blurring filters are shown.

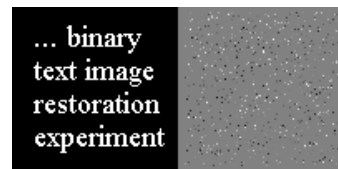


Figure 3: Left: text image. Right: star field.

The text image is blurred using the following two motion blur filters:

$$h_0[n, m] = \begin{cases} \delta[n - m] & \text{for } 0 \leq n, m \leq 5 \\ 0 & \text{elsewhere} \end{cases}$$

$$h_1[n, m] = \begin{cases} \delta[n] & \text{for } 0 \leq m \leq 5 \\ 0 & \text{elsewhere} \end{cases}$$

In Fig.4 the blurred text images are shown along with the deconvolved and the nonlinear MMSE estimated ones, for different signal-to-noise ratios (SNR) (both the channels have the same SNR): first row 10dB, second row 20dB, and third row 30dB. It is worth pointing out

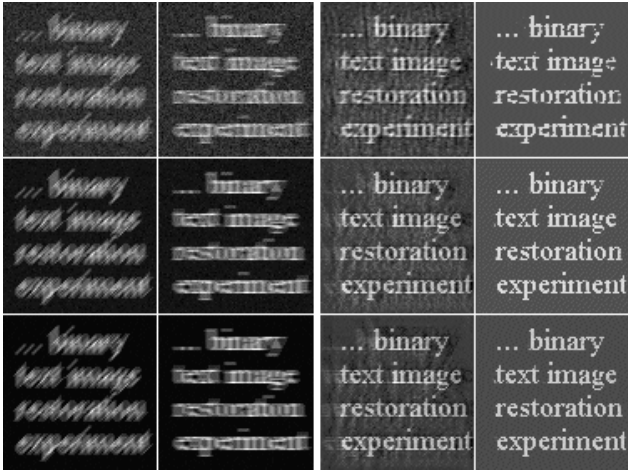


Figure 4: First and second column: blurred text images. Third column: deconvolved estimation $\hat{x}[m,n]$. Fourth column: nonlinear MMSE estimation $\tilde{x}[m,n]$

that the deconvolution technique here described allows obtaining clear and readable deconvolved text images. The iterative deconvolution converges after 30-35 iterations, as illustrated in Fig.5, where the MSE, as defined in (3), is plotted vs. the iteration number.

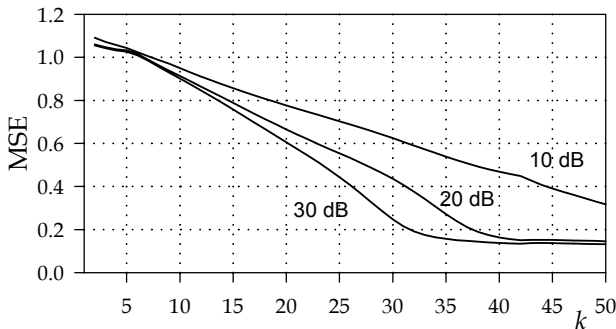


Figure 5: Binary text image deconvolution: MSE vs. iterations.

In Fig.6 the star field images blurred using four Gaussian shaped filters are shown. The impulse responses of employed blurring filters take the following form:

$$h_i[n, m] = e^{-[(n-n_i)^2+(m-m_i)^2]/2\sigma^2} \cdot \cos(\theta_i n) \cos(\phi_i m)$$

with $\theta_i/\pi = 0.2, 0.7, 0.2, 0.9$, $\phi_i/\pi = 0.1, 0.2, 0.9, 0.8$, $n_i = 0, 1, -1, 0$, $m_i = 0, 1, 0, 1$, and $\sigma = 3$. At the output of all the four filters we have SNR=10dB.

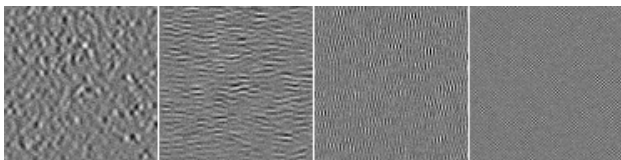


Figure 6: Blurred star fields at SNR=10 dB.

The deconvolved images are displayed in Fig.7. We see that the stars are clearly distinguishable after deconvolution, even those pairs that lie very close each other.

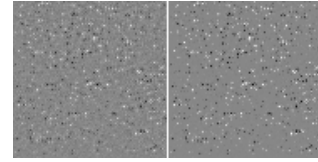


Figure 7: Restored star field image. Left: deconvolved estimation. Right: nonlinear MMSE estimation.

In this case convergence is attained after 20 iterations, as illustrated in Fig.8, where also the SNR values of 20, and 30dB have been reported for completeness.

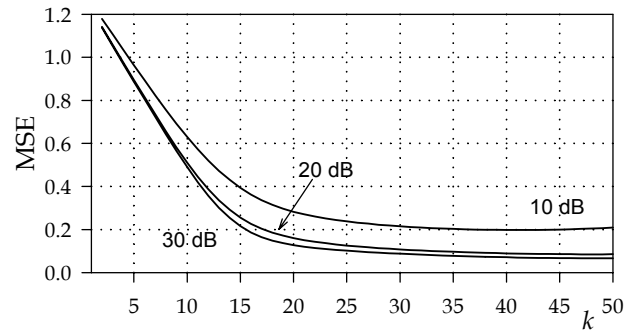


Figure 8: Star field image deconvolution: MSE vs. iterations.

References

- [1] A.K. Katsaggelos Ed., **Digital Image Restoration**, New York: Springer Verlag, 1991.
- [2] D. Kundur, D Hatzinakos, "Blind Image Deconvolution", *IEEE Sig. Proc. Mag.*, pp.43-64, May 1996.
- [3] "Special issue on blind systems identification and estimation," R. Liu and L. Tong, eds., *IEEE Proc.*, Vol.86, No.10, October 1998.
- [4] N.P. Galatsanos, V.Z. Mesarović, R. Molina, and A.K. Katsaggelos, "Hierarchical Bayesian Image Restoration from Partially Known Blurs", *IEEE Transactions on Image Processing*, Vol.9, No.10, pp.1784-1797, October 2000.
- [5] G. Harikumar, Y. Bresler, "Perfect blind restoration of images blurred by multiple filters: theory and efficient algorithm", *IEEE Transactions on Image Processing*, Vol.8, pp.202-219, February 1999.
- [6] G.B. Giannakis, R.W. Heath Jr., "Blind Identification of multichannel FIR Blurs and Perfect Image Restoration", *IEEE Trans. on Image Processing*, Vol.9, No.11, Nov. 2000.
- [7] R. Godfrey, F. Rocca, "Zero-memory non linear deconvolution," *Geophysical Prospecting*, 29, 1981.
- [8] S. Bellini, "Bussgang techniques for blind deconvolution and restoration," in **Blind Deconvolution**, S. Haykin ed., Prentice-Hall, 1994.
- [9] G. Jacovitti, G. Panci, G. Scarano, "Bussgang-Zero Crossing Equalization: An integrated HOS-SOS Approach", *IEEE Transactions on Signal Processing*, Vol.49, No.11, Nov. 2001.
- [10] P. Campisi, G. Scarano, "A multiresolution approach for texture synthesis using the circular harmonic function", *IEEE Transactions on Image Processing*, Vol.10, No.12, Dec. 2001.